Supporting Information

Solid-State Dynamic Nuclear Polarization at 9.4 and 18.8 T from 100 K to Room Temperature

Moreno Lelli,[1] Sachin R. Chaudhari,[1] David Gajan,[1] Gilles Casano,[2] Aaron J. Rossini,[3] Olivier Ouari,[2] Paul Tordo,[2] Anne Lesage,[1] Lyndon Emsley.[3,*]

[1]*Institut de Sciences Analytiques, Centre de RMN à Très Hauts Champs, Université de Lyon (CNRS/ENS Lyon/UCB Lyon 1), 69100 Villeurbanne, France;* [2]*Aix-Marseille Université, CNRS, ICR UMR 7273, 13397 Marseille, France.* [3]*Institut des Sciences et Ingénierie Chimiques, Ecole Polytechnique Fédérale de Lausanne (EPFL), CH-1015 Lausanne, Switzerland.*

Material and Methods

General Information. The *ortho*-terphenyl (OTP) and fully deuterated d_{14}-*ortho*-terphenyl were purchased from Alpha Aesar and Cambridge Isotope Laboratories, respectively. The stable radical BDPA (α,γ-bisdiphenylene-β-phenylallyl 1:1 benzene complex) was purchased from Sigma-Aldrich, while TEKPol was prepared according to the synthesis previously reported.[1-4] Deuterated polystyrenes were purchased from Polymer Source™. Ambroxol hydrochloride (4-[(2-amino-3,5-dibromophenyl) methylamino] cyclohexan-1-ol hydrochloride) was purchased from Sigma-Aldrich. Ibuprofen acid ((RS)-2-(4-(2-methylpropyl)phenyl)-propanoic acid) was purchased from Alfa Aesar.

DNP-NMR Methods. DNP-enhanced NMR experiments were performed using commercial Bruker 400 MHz and 800 MHz solid-state DNP-NMR spectrometers,[5,6] with Bruker Avance III consoles, and double or triple resonance 3.2 mm low-temperature CP-MAS probes. DNP is achieved by irradiating the sample with high-power microwaves at a frequency of 263 GHz for 9.4 T and 527 GHz for 18.8 T that are generated by two gyrotrons and are delivered to the sample through a corrugated wave-guide. The gyrotron operates continuously during the DNP-enhanced experiments (stability of better than ±1%). Sapphire rotors (with ZrO_2 caps) were used for optimal microwave penetration. Spinning frequencies were regulated to 8.0 kHz ± 2 Hz for all the experiments, excluding the DNP experiments on hydrated IBU-S crystals that were acquired at 7.0 kHz MAS and those on Ambroxol hydrochloride that were acquired at 13.0 kHz MAS

to reduce the overlap between the compound resonances and the rotational sidebands. The sample temperatures were varied from 100 to 300 K and determined, under microwave irradiation, by measuring the ^{79}Br T_1 relaxation times[7,8] of a small amount of KBr added to the rotor. Temperatures measured without microwave irradiation are generally 5-6 K lower at 9.4 T and 16-18 K lower at 18.8 T than the corresponding temperatures measured in presence of microwaves. This difference can generate a small error in the measurements of the enhancement (especially at 18.8 T and at low-temperature) that under-estimates the enhancement. The enhancement values were not corrected by this temperature factor. The ^{1}H and ^{13}C chemical shifts are referenced to TMS at 0 ppm.

^{1}H 1D direct excitation experiments were acquired with a rotor synchronized spin echo in order to suppress background signals. The pulse sequence was: $\pi/2$ — τ — π — τ — acquisition, $\pi/2$ and π pulses were calibrated at 2.5 μs and 5.0 μs (100 kHz), respectively. The τ delays were set to 1 rotor period. ^{1}H T_1 and DNP build-up times (T_B) were measured with a standard saturation recovery sequence followed by echo detection (saturation—$\tau_{recovery}$ — $\pi/2$ — τ — π — τ — acquisition) under microwave off and microwave on conditions, respectively. For temperatures above the glass-transition temperature (T_g, 243 K, –30 ˚C) the T_B build-up shows an almost bi-exponential trend with the presence of a minor, slow relaxing component. This minor component increases at higher temperature, and it is probably due to the formation of a crystalline OTP phase inside the sample. For these temperatures, the reported T_B values refer only to the major component that has the shorter relaxation times. Errors in the ^{1}H T_1/T_B were evaluated by repeating some measurements 3 or 4 times and evaluating the fluctuation of the fitted T_1/T_B values. We observed that T_B values below T_g have errors around ±4 %. Above T_g the error increases because of the uncertitude in fitting a biexponential trend and because of the instability of the melted phase. The ^{1}H T_1 measurements (without microwave), have lower signal to noise ratio and the error was estimated at about ±8-10 %.

Standard cross-polarization (CP) was used for the acquisition of 1D ^{13}C spectra. The recycle delay between scans was varied from 5.0 s to 70 s depending on the sample and the build-up time. For Solid-Effect enhancement experiments a

recycle delay of 60 s was used, and we observed that the enhancements do not appreciably change using longer recycle delays. Experimental values for ^{1}H echo-detected experiments, ^{1}H T_1/T_B and CP experiments at 400 MHz and 800 MHz are reported in Table S1.

Paramagnetic quenching was determined from the ratio of the intensities of ^{13}C OTP signal acquired with the same experimental parameters in presence and in absence of polarizing agent and without microwave irradiation. The weighed amount of sample (~17 mg) was confined to the more sensitive (central) region of the rotor with a PTFE insert. The ratio between the intensity of the spectra in presence and absence of radical was then scaled by the corresponding amount of effective sample.[1,9-12] For complete relaxation of the signal, recycle delays of 450 s, 250 s and 40 s were used for pure OTP, BDPA/OTP and TEKPol/OTP samples, respectively.

DNP enhancements (Table S4) were measured as the ratio of the NMR signal intensity of the solvent in presence and in absence of microwave irradiation. For all the samples, the NMR experiments were acquired after four cycles of insert/eject steps inside the spectrometer in order to remove traces of oxygen. The errors ($\Delta\varepsilon$) in the enhancements (ε) were evaluated with the following formula:

$$\Delta\varepsilon = \varepsilon\left(\frac{\Delta I_{(\mu w\ on)}}{I_{(\mu w\ on)}} + \frac{\Delta I_{(\mu w\ off)}}{I_{(\mu w\ off)}}\right) \quad (1)$$

where ΔI is the error in the intensity I of the observed peak (with and without microwave) and estimated on the basis of the noise level, imperfections in the baseline and the residual background signal that is not completely suppressed by the echo sequence. The relative errors are generally dominated by the measurement in absence of microwaves, they change with temperature on the basis of many factors (Boltzmann factor, Q-factor of the probe, ….). The absolute errors are generally higher for measurements with high enhancement factors, but for the sake of caution we report all the points on a curve with the largest observed error, even if this method generally overestimates the uncertainty. For the OE enhancement of BDPA in polystyrene, we found that the relative error is almost constant and the absolute errors scale with the enhancement. The

reported ^{1}H enhancements match well, within the experimental error, the ^{1}H enhancement measured though ^{13}C CP in the solvent peaks, and determined through the ratio of the integrated peak intensity with and without microwaves. Some representative ^{1}H-^{13}C CP MAS spectra at different temperature and at 18.8 T and 9.4 T are reported in Figures S6 and S7.

Note, we did not measure the SE enhancement in BDPA at 18.8 T because it is expected to decrease with the square of the magnetic field. Since at 9.4 T we observed SE enhancement of about 140, at 18.8 T and ~120 K we expect to have enhancements of about 35 that is much less of what we observed OE and CE at the same field.

Table S1. Experimental NMR parameters for ^{1}H echo-detected experiments, ^{1}H T_1/T_B and CP experiments at 400 MHz and 800 MHz

	400 MHz (9.4 T)	800 MHz (18.8 T)
^{1}H 1D echo-detected		
π/2 and π pulses	2.5 μs and 5.0 μs	2.5 μs and 5.0 μs
Acquisition time	4.0 ms	10.2 ms
Complex points acquired	400	1024
Exponential window function	250 Hz	200 Hz
^{1}H T_1/T_B		
Recycle delay (s)	0.5 s	0.5 s
π/2 and π pulses	2.5 μs and 5.0 μs	2.5 μs and 5.0 μs
Acquisition time	5.12 ms	10.2 ms
Complex points acquired	1024	1024
Exponential window function	250 Hz	200 Hz
{^{1}H}-^{13}C Cross Polarization		
^{1}H π/2 pulse	2.5 μs	2.5 μs
Contact time (τ_{CP})	2.5 ms	1.5 ms
Linear Ramp	70 % to 100 %	70 % to 100 %
CP power level ^{1}H	75.5 kHz	76.5 kHz

^{13}C	43.0 kHz	71.36 kHz
^{1}H Decoupling (SPINAL-64)[9,10,13,14]	100 kHz	100 kHz
Acquisition time	16.08 ms	10.2 ms
Complex points	804	994
Line broadening	400 Hz	400 Hz

Table S2. Experimental NMR parameters for ^{1}H-^{13}C CP experiments acquired at 9.4 T on Ambroxol hydrochloride and IBU-S impregnated with OTP/TEKPol.

{^{1}H}-^{13}C Cross Polarization (400 MHz -9.4 T)	
^{1}H $\pi/2$ pulse	2.12 μs
Contact time (τ_{CP})	2.0 ms
Linear Ramp	50 % to 100 %
CP power level ^{1}H ^{13}C	 110.0 kHz 54.8 kHz
^{1}H Decoupling (SPINAL-64)[9,13]	123 kHz
Acquisition time	29.29 ms
Complex points	1024
Line broadening	80 Hz

Sample Preparation.

OTP sample preparation.

OTP samples were prepared by dissolving the polarizing agent (32 mM BDPA (α,γ-bisdiphenylene-β-phenylallyl) or 16 mM TEKPol) in a mixture of 95% OTP-d_{14} and 5% OTP. We used the same level of deuteration that had been optimized in ref. [9,15]. The concentration of TEKPol (16 mM) was the same as reported[2,9] for tetrachloroethane (TCE), which is close to the optimal values observed for bi-nitroxide polarizing agents in several solvents.[1-4] The BDPA concentration was 32 mM in order to have the same unpaired electron concentration as the TEKPol sample, and this concentration is not far from the concentration reported in the

literature for Overhauser effect and Solid-Effect DNP on SA-BDPA[5,6] (40 mM). The concentrations and deuteration levels were not optimized further.

Both the polarizing agent and the OTP mixture were dissolved in ~1 mL of deuterated chloroform and after homogenization of the solution the solvent was allowed to evaporate on a glass plate. The resulting solid powder was then packed into the sapphire rotor. The OTP powder was then melted in the rotor at about 338 K (65 ˚C), and then rapidly frozen after insertion into the cold NMR probe to obtain the glassy frozen OTP phase.

During the process of evaporation of the chloroform it is possible that the OTP crystallizes and aggregation/clustering of the polarizing agent cannot be excluded. Before inserting the sample into the cold probe, the OTP is thus melted inside the rotor for a sufficiently long time (generally 2-5 min) to ensure the homogeneous dissolution of the polarizing agent. Preparing the sample in absence of paramagnetic oxygen or storing the sample under N_2 also helps in obtaining high enhancements and longer ^{1}H T_B. The difficulty in degassing the different OTP phases and in controlling the homogeneous dissolution of the radical can affect the reproducibility of the enhancements. BDPA/OTP samples are generally more sensitive to improper preparation than TEKPol/OTP. Following this procedure, at ~115 K and 9.4 T, OE enhancements of the order of 60-90 and OE ^{1}H T_B around 35-55 s are reproducible. The enhancement and ^{1}H T_B temperature profiles reported in figures 1 and S5 represent profiles that we reproduced on several samples and on different batches of polarizing agent.

For the above reasons, the enhancements reported for analogous temperatures in Table S3-S4, Figure 1, Figure S5 and Figure S1 show small differences. SE enhancement up to 180 at 115 K was also observed in one sample, and for this reason we cannot exclude that an improvement in the sample preparation is still possible. An EPR investigation at 263-527 GHz could help in the understanding of these processes and will be the subject of a further study.

A procedure similar to that used to prepare OTP samples was followed to prepare the BDPA solution (2% w/w) in highly deuterated polystyrene (~190 kDa, 95% poly-(styrene-d_8), 5% poly-(styrene-d_5)) but in this case, the polystyrene film obtained after evaporation of chloroform was ground, kept

overnight under vacuum to remove remaining solvent, and then packed into the rotor and directly inserted into the low-temperature probe.

Behavior above the OTP glass transition.

At the glass transition the DNP enhancements and T_B (and T_1) rapidly drop. The effect is more pronounced at 9.4 T than 18.8 T for both OE and CE (Figure S5). Many factors are involved. The increased dynamics in proximity of T_g and in the melted metastable phase reduce T_1 (especially in presence of paramagnetic species), as well as the T_B, the enhancements, the spin-diffusion processes, etc…. This is probably the main reason for the rapid drop of these parameters "at T_g" and the effect, especially on T_1 could be different at different magnetic fields. Just above T_g, the crystallization process occurs and aggregation/clustering of the polarizing agent is also possible, especially with increasing temperature and reduced viscosity of the solvent. In absence of accurate EPR data at 263-527 GHz it is difficult to establish the relative role of these processes and to unravel the reason of the different behavior observed at 9.4 T and 18.8 T. The characterization of this phenomenon will be a matter of further investigation.

IBU-S sample preparation.

Hydrated Ibuprofen sodium salt (sodium (RS)-2-(4-(2-methylpropyl)phenyl)-propanoate dihydrate) here referred to as IBU-S was prepared from Ibuprofen acid ((RS)-2-(4-(2-methylpropyl)phenyl)-propanoic acid) after titration with an aqueous solution of sodium hydroxide. The hydrated salt was obtained by crystallization after water evaporation. To ensure the correct hydration level the crystals were kept under atmospheric humidity for at least 4 hours, as previously reported.[7,8] The DNP sample was prepared by grinding together IBU-S crystals and a previously prepared solid solution of 16 mM TEKPol in OTP. The mixed powder was than packed into a 3.2 mm sapphire rotor. The rotor contained 5.5 mg of KBr packed in the bottom, 5.8 mg of OTP/TEKPol powder, and 20.3 mg of IBU-S sample. OTP was then melted inside the rotor keeping it at the temperature of 333-338 K (60-65 ˚C) for 3 minutes, in order to obtain the uniform wetting of the IBU-S crystals, and it was then rapidly inserted in the cold DNP probe. Solution NMR spectra performed by suspending IBU-S powder in a

molten OTP sample at 338 K (65 ˚C) clearly showed that IBU-S is not soluble in molten OTP, and that thus OTP is a suitable non-solvent.

Ambroxol hydrochloride sample preparation.

The DNP sample was prepared by grinding together Ambroxol crystals and a previously prepared solid solution of 16 mM TEKPol in OTP. The mixed powder was than packed into a 3.2 mm sapphire rotor. The rotor contained 5.8 mg of KBr packed in the bottom, 10.4 mg of OTP/TEKPol solution and 21.2 mg of Ambroxol hydrochloride. OTP was then melted inside the rotor at 333-338 K (60-65 ˚C) as for IBU-S and was then rapidly inserted into the cold DNP probe. Solution NMR spectra performed by suspending Ambroxol powder in molten OTP at 338 K (65 ˚C) confirmed that OTP does not solubilize Ambroxol and can be used as a non-solvent.

DNP characterization of the organic compounds of pharmaceutical interest: Ambroxol hydrochloride and hydrated Ibuprofen sodium salt.

DNP has been successfully applied to the characterization of organic compounds and pharmaceutical preparations.[1,9-12] One of the most successful DNP approaches consists in impregnating the microcrystalline powder of the organic compounds with a solution of the polarizing agent. If the medium (for example OTP) is chosen in order not to solubilize the organic compound (non-solvent), the polarizing agent solution will just impregnate the surface of the microcrystalline grains. Under DNP conditions and upon microwave irradiation, the protons of the glass-frozen solvent are rapidly hyperpolarized and the polarization can then penetrate into the microcrystals by means of the proton-proton spin diffusion.[9,10,13,14] The enhanced proton polarization inside the microcrystals is then transferred to carbon by ^{1}H-^{13}C Cross-Polarization (CP), making possible to obtain ^{13}C spectra of the organic compound with DNP enhancements up to 60-70. This allows one to acquire, for example, ^{13}C-^{13}C correlation spectra at natural isotopic abundance.[9,13] Since the polarizing agent is present only at the surface of the particles, effects like increased resonance broadening or paramagnetic bleaching are very limited.[9,15] The overall signal intensity and the DNP enhancement depend not only on the nature of the

polarizing agent and the solvent, but they also depend on the substrate (that determines the ^{1}H T_1 and the proton spin-diffusion constant) and on the size of the microcrystals. These parameters affect the penetration of the hyperpolarization into the particles. Interestingly, this approach works best with organic compounds having long ^{1}H T_1 (which allows for a deeper polarization inside the crystal) that are generally difficult to investigate with traditional ssNMR due to the long recycle delay.[2,9]

Here we demonstrate that OTP/TEKPol can be used as a polarizing matrix for DNP hyperpolarization of microcrystalline organic compounds over variable temperatures in the range 100-240 K below the glass-transition temperature of OTP. To demonstrate this we investigated two organic compounds of pharmaceutical interest: Ambroxol hydrochloride[16] and hydrated Ibuprofen sodium salt.

Figure S4 shows the DNP MAS ssNMR spectra (9.4 T and 13.0 kHz MAS) of microcrystalline Ambroxol hydrochloride impregnated with 16mM TEKPol in OTP from 113 to 236 K. At 113 K the enhancement in the OTP signal is greater than 150 ($\varepsilon_{C\_CP\_OTP} > 150$) but is difficult to measure because of the weak signal of the solvent in the spectrum without microwaves and the overlap with the Ambroxol resonances. The enhancements on the overall proton resonances (Ambroxol + OTP) was $\varepsilon_H = 138$, and the enhancement detected through CP on the Ambroxol resonances was ε_{C_CP} (Ambroxol) = 54. These values are not optimized, higher enhancements and absolute signals may be obtained by optimizing the polarization delay (recycling time) or the particle size of the ground powder.[9] The polarization delay in the present spectra was set to 10 s to allow one to acquire the DNP enhanced spectrum in less than 6 minutes. With increasing temperature the DNP enhancement decreases (as expected), but we can still observed Ambroxol signal enhancements larger than 20 at 189 K and of 8 at 236 K (–36.7 ˚C). This corresponds to a reduction of the overall acquisition time by a factor 64 compared to the spectrum acquired without microwave at 236 K. This demonstrates that the OTP/TEKPol mixture can be used as an efficient polarizing medium for the characterization of organic microcrystalline compounds with DNP over a large range of temperatures.

As a second example, we report the DNP investigation of the microcrystalline Ibuprofen sodium salt (IBU-S) in the temperature range from 107 K to 225 K. IBU-S is known to undergo to several dynamical processes inside the crystal, with flipping of the aromatic ring, dynamics of the isopropyl group and rotation of the methyl groups.[7,17,18] These dynamical processes have recently been characterized over a large range of temperature (from 20 K to 358 K) by solid-state NMR using standard and low-temperature MAS probes.[7] Concistrè *et al.* showed that in the range from 60 K to 260 K many changes in the ^{13}C CP-MAS spectra are observable, especially in the aliphatic region, because of the freezing of the isopropyl and methyl rotation dynamics. Figure 2 (main text) shows the DNP enhanced ^{13}C CP MAS spectra we acquired for IBU-S microcrystals impregnated with 16 mM TEKPol in OTP. The overall proton enhancement (OTP + IBU-S) at 107 K is $\varepsilon_H = 180$ while the enhancement measured through CP in the IBU-S resonance is about ε_{C_CP} (IBU-S) ~10.[19] The difference in the enhancement between the IBU-S and the overall protons indicates that the hyperpolarization penetrates less the crystals with respect to that observed for Ambroxol, which could be related to the possibly larger size of the microcrystals or more likely to the rotational dynamics of the three methyl groups that act as relaxation sinks and reduce the efficiency of proton-proton spin diffusion, as previously observed for paracetamol or theophylline.[9,20,21] However, shorter relaxation times allow faster repetition, which partially compensates for less efficient DNP.(Ref [9]) An enhancement of ~10 corresponds to an acceleration by a factor 100 in acquisition time, and makes possible to clearly observe the dynamical process at different temperatures, especially in the temperature range between 100-160 K where the broadening of many resonance made them hardly detectable without DNP.[7] At temperatures above 157 K the progressive increase of the isopropyl and methyl conformational dynamics lead to a visible narrowing of the resonances in the aliphatic region. This process has been well described previously[7,17] and will be not further detailed here. Comparing the present spectra with the previously reported spectra[7] we observe analogous changes in the NMR spectra that correspond well but with a gap of about 20-40 K. This difference is probably related to different preparation of the IBU-S salt, and

possibly to small differences in the degree of moisture/hydration level in the IBU-S powder, which can partially affect the dynamics in the crystal. In ref [7], the spectra below 120 K were acquired at 14.1 T instead of 9.4 T, this also might in part justify the observed differences. (Note that the peaks at about 170 ppm are probably either a minor second form or trace impurities.)

All these results show that the variable temperature DNP approach proposed here is effective to monitor dynamic processes in microcrystalline organic compounds. The high sensitivity of the DNP NMR technique makes also possible to acquire deuterium NMR spectra in microcrystalline organic compounds at natural isotopic abundance.[21] Thus, with the method proposed here, dynamical information could also be obtained from the analysis of ^{2}H NMR spectra acquired over a range of temperatures.

Supplementary Description of the Solid-Effect, Overhauser-Effect Enhancements and DNP build-up Time.

Solid effect (SE)

The theoretical description of the solid-effect (SE) has been developed by several authors, with equations that only slightly differ depending on the approximations introduced in describing the electron-nuclear hyperfine relaxation, the spin-diffusion barrier, the proton spin diffusion mechanism or other details in the SE-DNP mechanism.[22-29] For the reader's convenience we present a short summary here.

Abragam and Goldman[23,24] reported an equation for SE-DNP where the enhancement ε_{SE} and the build-up time T_B are scaled by the saturation factor s and the leakage factor f. These equations, also summarized in ref. [30] show that:

$$\varepsilon_{SE} = \left(\frac{\gamma_e}{\gamma_n}\right)\frac{1}{1+\alpha f+f/s} \tag{2}$$

$$\frac{1}{T_B} = \frac{1}{T_{1n}^0}\left(f + \frac{s}{1+\alpha s}\right) \tag{3}$$

where

$$f\alpha = \alpha\left(\frac{T_{1n}^0}{T_{1n}'}\right) = \left(\frac{N_n}{T_{1n}'}\right)\left(\frac{T_{1e}}{N_e}\right) \tag{4}$$

$$\alpha = \frac{2\pi}{5}\left(\frac{\gamma_e}{\gamma_n}\right)\left(\frac{\Delta B_n}{B_0}\right)^2 \tag{5}$$

$$s = \pi(\gamma_e B_1)^2 g(\omega) T_{1e};\ \ \omega = 0 \tag{6}$$

where γ_e and γ_n are the electron and nuclear gyromagnetic ratio, respectively, B_0 is the external magnetic field, ΔB_n is the proton linewidth in the solid, B_1 is the strength of the microwave power, $g(\omega)$ is the shape of the EPR linewidth normalized to the unit area and centred in $\omega = 0$. N_e and N_n are the number of unpaired electrons and proton nuclei per volume in the sample, T_{1e} is the electron longitudinal relaxation time, the leakage factor f is the ratio between the expected nuclear longitudinal relaxation time in case of relaxation by only the electron-nuclear hyperfine interaction (T_{1n}^0) and the effective proton relaxation when also other relaxation mechanism are operative (T_{1n}').

Equation 2 clearly indicates that in the SE the DNP build-up time is related to the nuclear T_1 time but is different from it, and also depends on the microwave power through the saturation factor.

Wind *et al.* [31,32] re-wrote the SE enhancement in an approximated but more practical formula:

$$\varepsilon_{SE} = \lambda \left(\frac{\gamma_e}{\gamma_n}\right) \frac{N_e}{b^3 \delta} \left(\frac{B_1}{B_0}\right)^2 T_{1n}' \qquad (7)$$

where λ contains physical constants, b is the radius of the spin diffusion barrier and δ is the width of the EPR lineshape. This equation has the advantage to clearly predict a linear dependence of the solid-effect enhancement on the nuclear relaxation time, showing that higher enhancements should be obtained with longer proton relaxation times.

Recently, Griffin[25,26] and coworkers and Vega[27] and coworkers independently reinvestigated the solid-effect considering differently the role of the spin-diffusion barrier and the spin-diffusion processes from a core of nuclei close to the radical to the nuclei in the bulk. All their simulations clearly demonstrated, among others, that the SE enhancement increases with increasing microwave power and nuclear T_1, and that the DNP build-up time ^{1}H T_B also depends on the microwave power and is generally shorter than ^{1}H T_1.

Comparison between ^1H T_1 and ^1H T_B in Solid effect and Overhauser effect DNP

The equations reported in the previous section show that SE ^1H T_B can significantly differ from ^1H T_1, depending on the microwave power applied. Conversely, for the Overhauser effect we observed that the ^1H T_B matches well the ^1H T_1 within the limits of the experimental error (Table S3), as also previously observed.[5]

Table S3. Experimental OE DNP ^1H T_B and ^1H T_1 measured at different temperatures together with the observed ^1H enhancement. The values are measured on a sample of 32 mM BDPA in 95% deuterated OTP at 9.4 T. The experiment was run with 2 and 16 scans for ^1H T_B and ^1H T_1, respectively. The ^1H T_B and ^1H T_1 experiments were run at the same temperature compensating the heating of the experiment with microwaves.

Temperature (K) (error ±1.5 K)	ε_H	^1H T_B (s)	^1H T_1 (s)
112	64	48 ± 2	44 ± 4
155	67	37 ± 2	37 ± 4

Within the experimental error the OE DNP ^1H T_B is equal to the ^1H T_1.

Since the SE DNP ^1H T_B is different from the ^1H T_1 we can thus explain why the build-up times measured with the same sample for the OE or the SE conditions are different (Figure S5). However, equations (3) and (8) show that SE enhancement and T_B are also a function of the proton T_1, and consequently they follow the same trend and the same drop above T_g.

Overhauser effect (OE)

The Overhauser DNP effect in solid insulators has been clearly observed up to now only for BDPA and the water soluble SA-BDPA derivative, [5,33] and a comprehensive theoretical description of the phenomenon is, at the moment, not available. The first OE DNP observed for BDPA dispersed in polystyrene showed an enhancement that scales with the magnetic field. Dissolving BDPA in OTP we observe that the enhancement remains substantially the same at 9.4 T and 18.8 T. Furthermore we observe that the temperature profiles for the OE at 9.4 T and

18.8 T are different and are not simply the same curve "scaled by field". We do not have detailed explanation for this phenomenon, that would require more experimental data and in particular EPR data up to 18.8 T, and is well outside the scope of the present work. We can propose some theoretical considerations in order to interpret the differences in the experimental OE temperature profiles observed at 9.4 T and 18.8 T (Figure 1 and Figure S5). We use the available theory of the Overhauser Effect (OE) in non conducting samples (most of them refer to solution OE) that has been described in many reviews,[22,31,34-36] and is expected to be applicable to some extent also in solid insulators.[5,31,33]

The considerations derived here are indicative and should be validated by more experimental data in the future, including EPR data at different fields and temperatures, and for different OE polarizing agents. Tests on different OE polarizing agents are also important to discern how the observed phenomena are related to the OE effect itself or to a combination of other more specific properties of the BDPA radical.

The general expression for the OE enhancement for a system composed by one nucleus and one electron (Scheme S1) is:

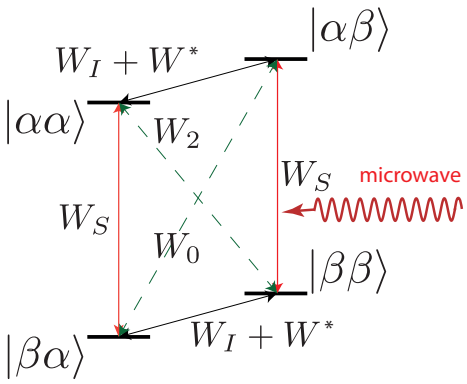

Scheme S1. Scheme of the transition pathways in an electron-nucleus two spin system.

$$\varepsilon_{OE} = 1 - sf\xi\frac{|\gamma_e|}{\gamma_n} \tag{8}$$

$$s = \frac{S_0 - \langle S_z\rangle}{S_0} = \frac{\gamma_e^2 B_1^2 T_{1e} T_{2e}}{1+\gamma_e^2 B_1^2 T_{1e} T_{2e}} \tag{9}$$

$$f = \frac{\rho_I}{\rho_I + W^*} = \frac{W_0 + 2W_I + W_2}{W_0 + 2W_I + W_2 + W^*} \tag{10}$$

$$\xi = \frac{\sigma_{IS}}{\rho_I} = \frac{W_2 - W_0}{W_0 + 2W_I + W_2} \tag{11}$$

where s is a saturation factor accounting for the non incomplete saturation of the electron transition by microwaves and, assuming the electron obeys the Bloch equations, it is a function of the microwave power B_1 and the longitudinal and transverse electron relaxation times T_{1e}, T_{2e}. f is a leakage factor that takes into account the reduction of the total enhancement due to other nuclear relaxation terms W^* that are not related to the electron-nucleus hyperfine interaction. ξ is coupling factor that describes the Overhauser effect, i.e. the ratio between the cross-relaxation (σ_{IS}) and the auto-relaxation terms (ρ_I), and depends on the DQ, SQ and ZQ relaxation probabilities (W_2, W_1, W_0, respectively).

The expression proposed for the saturation factor is strictly valid only for static samples. Under magic angle spinning and in presence of electron-electron spin exchange the formal description is significantly more complicated and we do not report it here. Can *et al.* pointed out that the electron spin transition for BDPA in polystyrene can be saturated with just ~3-4 W of microwave power at 9.4 T and ~100 K.[5] If at ~100 K commonly used microwave power is sufficient to saturate the EPR line, this condition might not be respected at higher temperatures where the electronic relaxation times are expected to be shorter, or at higher field than 9.4 T. It could be possible that at 18.8 T the EPR line is less saturated than at 9.4 T, and increasing the temperature the saturation level could decrease faster at 18.8 T than 9.4 T generating the rapid decrease observed in Figure 1B. Finally the saturation factor could be reduced in the presence of aggregation of the polarizing agent (for example during the crystallization of the OTP in the metastable phase) that would significantly affect the electronic relaxation times.
The leakage factor f accounts for the reduction in enhancement due to the presence of other nuclear relaxation processes in addition to the direct proton electron hyperfine interaction. This term has been used in solid-state DNP theory by Abragam and Goldman[23,24], even if the detailed formal description would be quite complicated, especially in solid-state MAS NMR. This term can play an important role in the OE DNP: for example it can be responsible of the reduction of enhancement, or of the problem in reproducibility of the enhancement in samples that are not completely degassed from oxygen or where the polarizing agent is not perfectly solubilized. Finally it could also be responsible of the rapid

decrease of the enhancement above T_g. In the metastable phase formed above T_g the increased mobility as well as the aggregation of the radicals will lead to the rapid reduction of the bulk ^1H T_1 and to the consequent reduction of *f*. Since the bulk ^1H T_1 is also dependent on the magnetic field and indirectly also on the electronic relaxation times of the radical, the leakage factor can also play a role in understanding the differences between the temperature OE profiles at 9.4 T and 18.8 T.

The coupling factor describes the Overhauser Effect, which is driven by the DQ and ZQ transitions in presence of a stochastic modulation of dipolar or scalar hyperfine interactions.

In case of the simultaneous presence of dipolar and scalar relaxation mechanisms, the following expression for ξ can be found:[34]

$$\xi = \frac{6J_{d_2}(\omega_I+\omega_S)-J_{d_2}(\omega_I-\omega_S)-5MJ_{s_2}(\omega_I-\omega_S)}{6J_{d_2}(\omega_I+\omega_S)+J_{d_2}(\omega_I-\omega_S)+3J_{d_1}(\omega_I)+5M\{J_{s_2}(\omega_I-\omega_S)+\beta\, J_{s_1}(\omega_I)\}} \tag{12}$$

where the spectral densities usually are:

$$J_{d_i}(\omega) = \frac{\tau_{d_i}}{1+\omega^2\tau_{d_i}^2}, \qquad i = 1,2$$

$$J_{s_i}(\omega) = \frac{\tau_{s_i}}{1+\omega^2\tau_{s_i}^2}, \qquad i = 1,2$$

$$\tau_{s_1} = (1/\tau_e + 1/\tau_1)^{-1} \qquad \tau_{s_2} = (1/\tau_e + 1/\tau_2)^{-1} \tag{13}$$

where τ_d and τ_s are the correlation times for the dipolar and scalar relaxation mechanism, while M is the constant ratio of the scalar and dipolar couplings. The correlation time τ_e refers to the electron spin-exchange, while the correlation times τ_1 and τ_2 correspond to the longitudinal and transverse electron relaxation times (assuming the validity of the Bloch equations for the electron). The term β is a factor measuring the relative contribution of scalar relaxation of the first kind with respect to scalar relaxation of the second kind, as it is reported by Abragam. [22,34]

The OE observed in insulating solids is dominated by scalar relaxation, and generates positive DNP enhancements.[5] Neglecting any dipolar contribution in the above expression for ξ we obtain:

$$\xi = \frac{\sigma_{IS}}{\rho_I} = \frac{-J_{S_2}(\omega_I - \omega_S)}{J_{S_2}(\omega_I - \omega_S) + \beta\, J_{S_1}(\omega_I)} \qquad (14)$$

In the hypothesis that scalar relaxation of the first kind is the only source of relaxation ($\beta = 0$), only the ZQ transition (W_0) is possible and the OE is constantly $\xi = -1$.[34] In this limiting case the coupling factor is independent of the magnetic field and the correlation time (τ_s), and consequently it is also independent of temperature. Even in this limiting case the overall enhancement can still conserve a temperature dependence inside the saturation and the leakage factors. In a more realistic situation the coupling factor could also contain small contributions due to scalar relaxation of the second kind or dipolar relaxation terms that can reintroduce a partial temperature dependence. A detailed characterization of the electronic properties by EPR is required to unravel all these possible situations, but in some circumstances it is possible that OE DNP is intrinsically less dependent on the temperature than the SE or the CE, as it could be the case described in Figure S3.

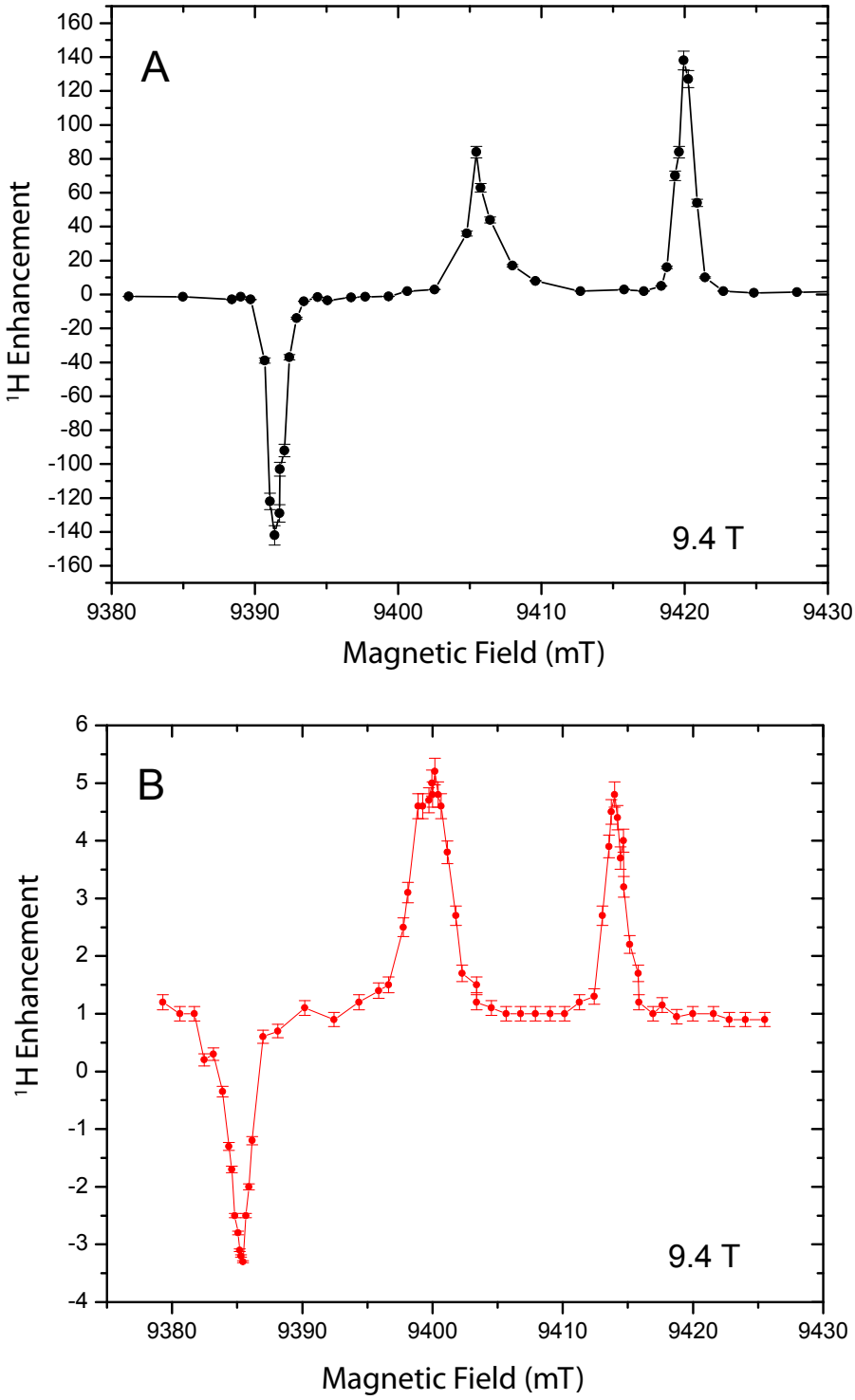

Figure S1. Magnetic field-dependence of the ^{1}H DNP enhancement for 32 mM BDPA in OTP (95% OTP-d_{14}, 5% OTP) (A, black curve) and tetrachloroethane (B, red curve), at 9.4 T and 112 K. Differences in the positions of OE and SE transitions in the OTP and TCE profiles are because they were acquired on DNP instruments working at slightly different microwaves frequencies.

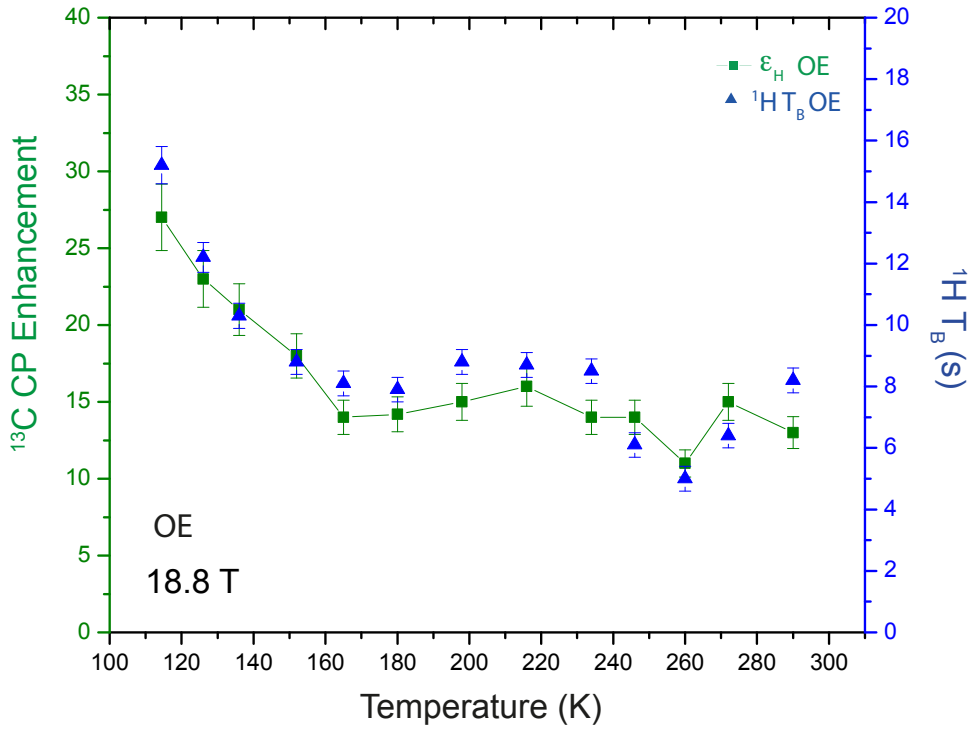

Figure S2. Bulk ^{1}H OE DNP enhancement (green squares) and ^{1}H DNP T_B (blue triangles) of highly deuterated polystyrene (95% poly-(styrene-d_8), 5% poly-(styrene-d_5)) with 2% BDPA at 18.8 T. The ^{1}H enhancement was measured by detecting the ^{13}C signal after ^{1}H-^{13}C cross-polarization.

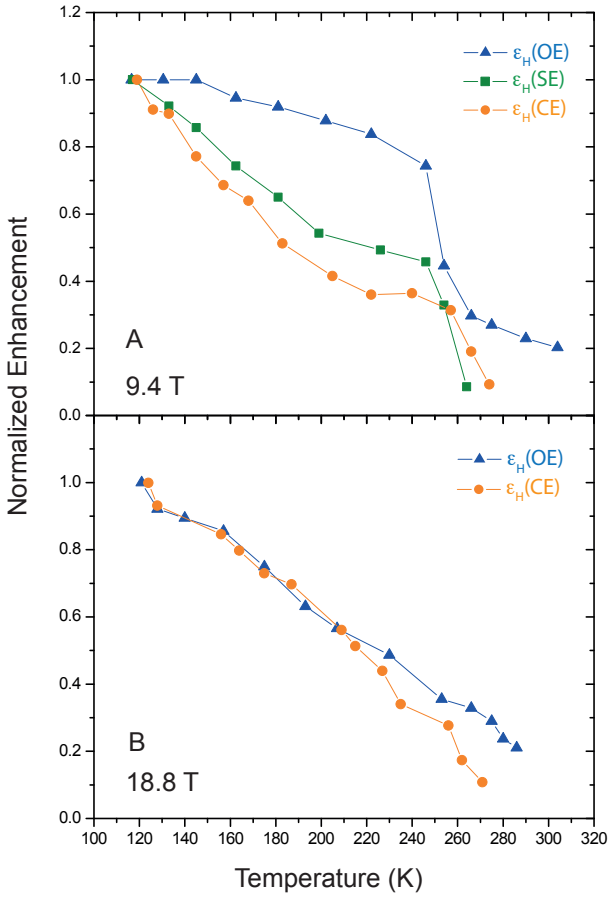

Figure S3. Temperature dependence of normalized enhancements for SE, OE, CE at 9.4 T (A) and 18.8 T (B). These are scaled versions of the enhancements reported in Figure 1 (main text), the enhancement curves are normalized by setting to 1.0 the value measured at the lowest temperature.

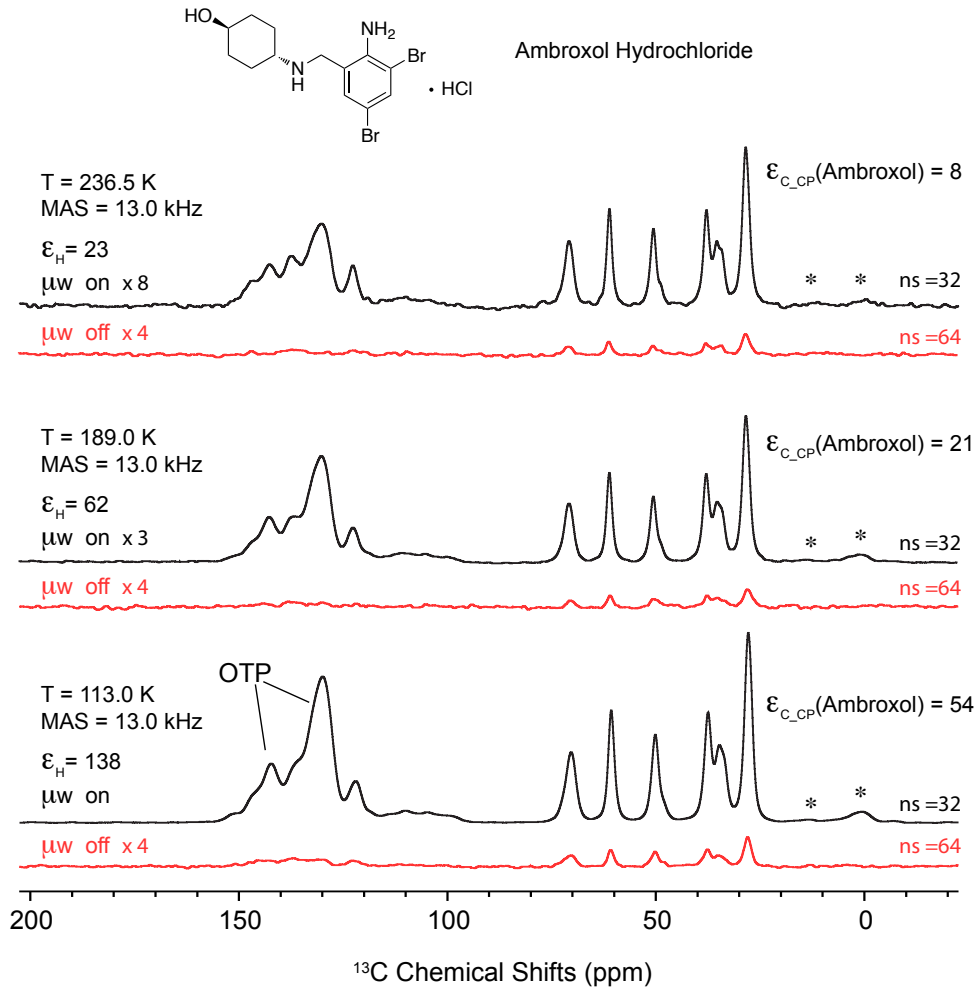

Figure S4. ^{13}C CP DNP MAS spectra at different temperatures of microcrystalline Ambroxol impregnated with 16 mM TEKPol in OTP (95% OTP-d_{14} and 5% OTP). The temperature was monitored in presence of microwaves by measuring the ^{79}Br T_1 of KBr crystals[8] added to the sample. The spectra were acquired at 9.4 T with 13.0 kHz MAS. The recycle delay was 10 s for all the spectra. The "μwave on" spectra were acquired with 32 scans while for the spectra without microwave 64 scans were used. Stars correspond to sideband peaks from OTP. Other experimental details are given in the experimental section.

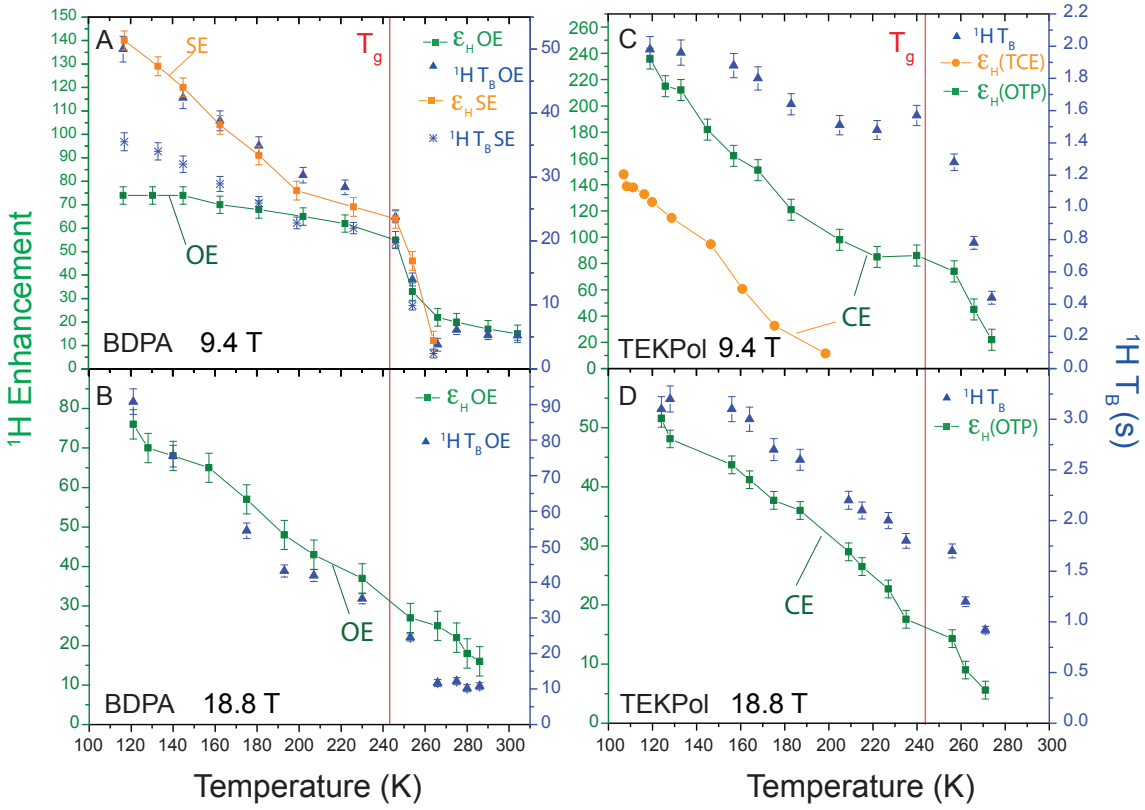

Figure S5. ^{1}H DNP enhancements (squares) and ^{1}H build-up times T_B (triangles, stars) as a function of temperature for 32 mM BDPA in 95% OTP-d_{14} for (A) SE and OE DNP at 9.4 T and (B) OE DNP at 18.8 T, as well as for 16 mM TEKPol in OTP at (C) 9.4 T and (D) 18.8 T. Enhancements previously measured for TEKPol in TCE at 9.4 T (ref. [2]) are reported for comparison (circles) in (C). The red lines indicate T_g. Numerical values are given in Table S4 for all the points.

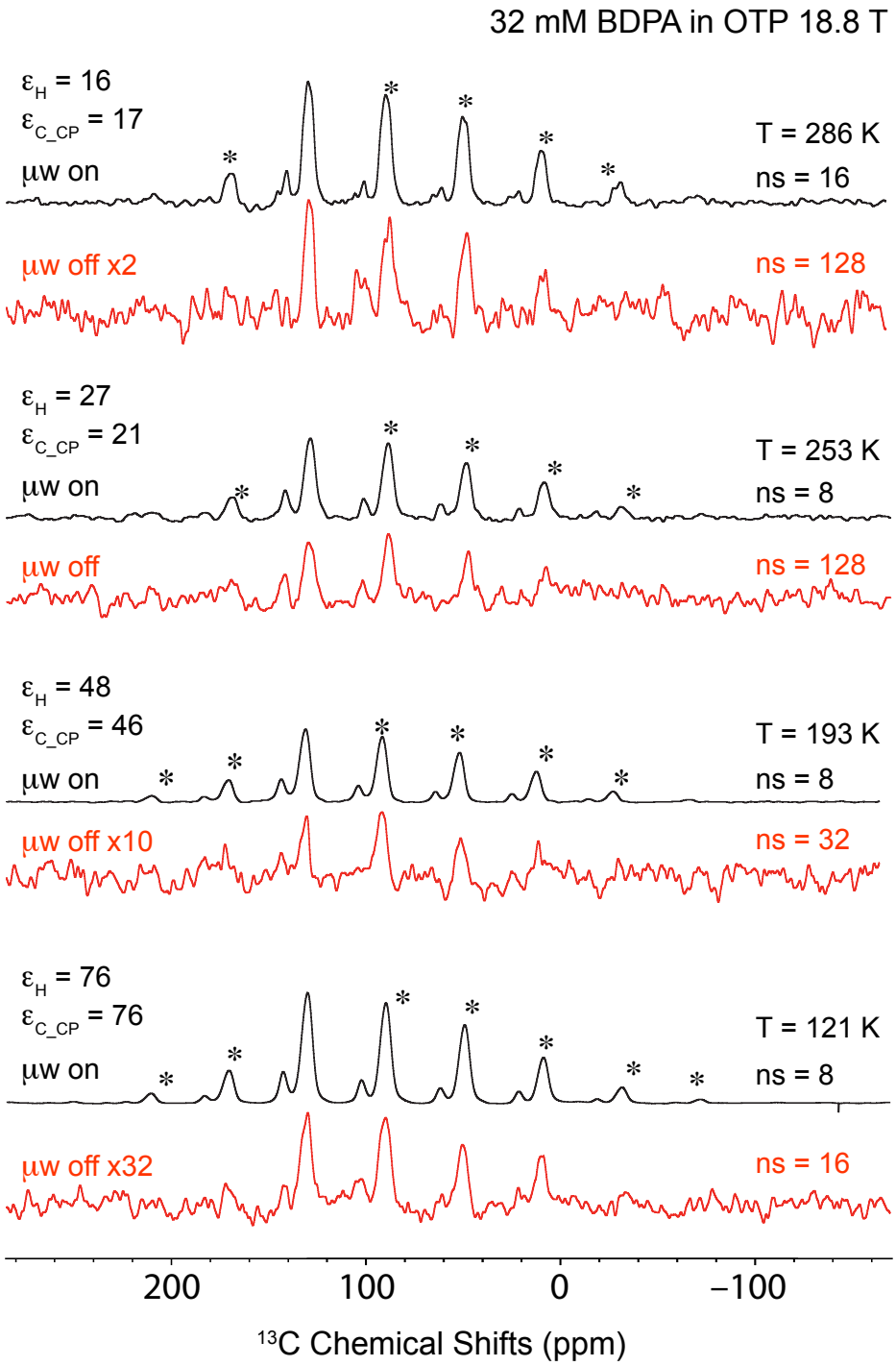

Figure S6. Selection of DNP-enhanced ^{1}H-^{13}C CP MAS spectra at different temperatures of a sample of 32 mM BDPA in OTP (95% OTP-d_{14} and 5% OTP) at 18.8 T. Stars indicate spinning sidebands.

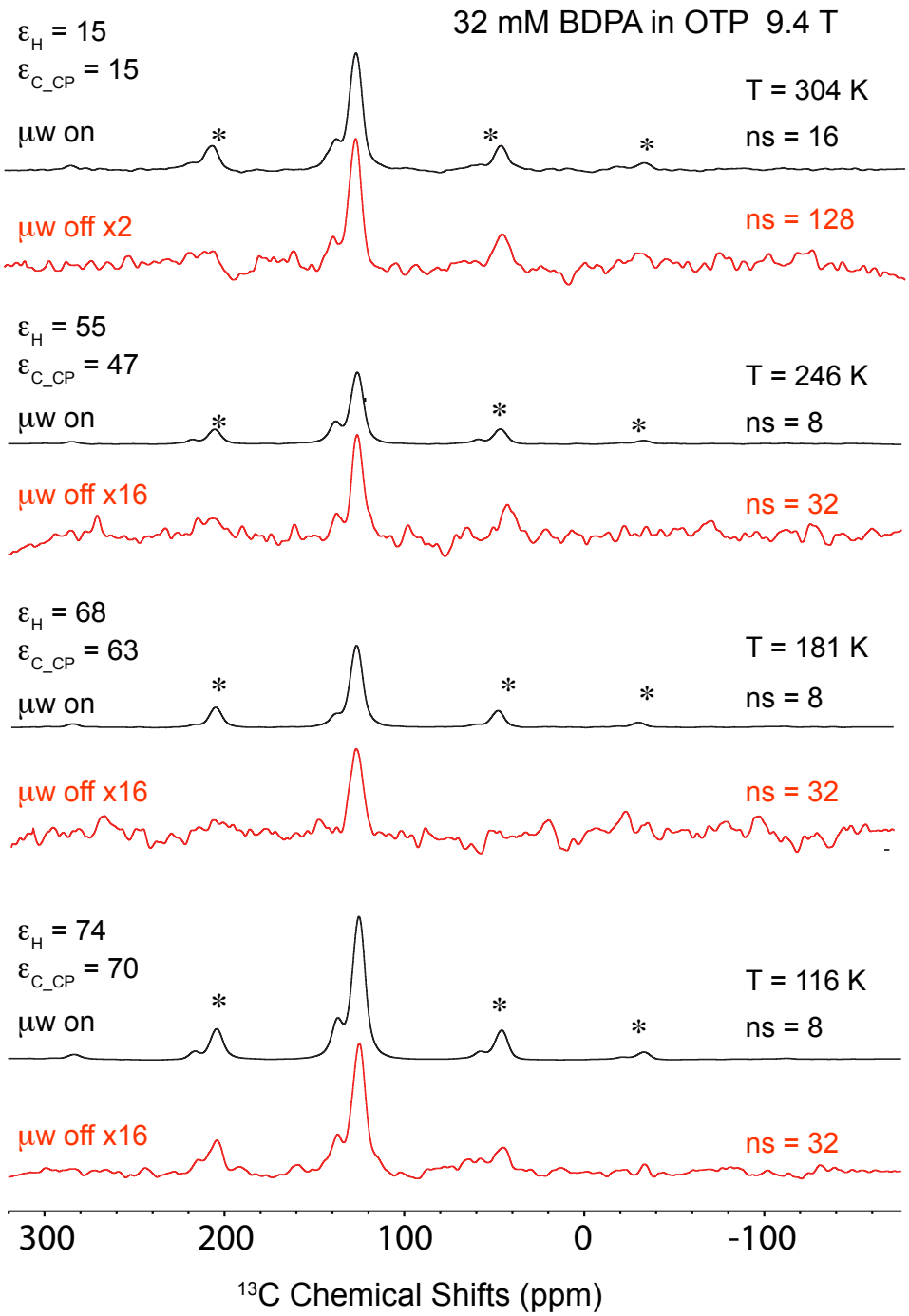

Figure S7. Selection of DNP-enhanced ^{1}H-^{13}C CP MAS spectra at different temperatures of a sample of 32 mM BDPA in OTP (95% OTP-d_{14} and 5% OTP) at 9.4 T. Stars indicate spinning sidebands.

Table S4. Experimental DNP enhancements and Build-up times (^{1}H T_B) measured at different fields for the different DNP mechanisms (these data are plotted in the Figures 1 in the main text).

BDPA OE at 9.4 T			
Temperature (K)	^{1}H Enhancement	Error (±)	^{1}H T_B
116.5	74	4	50
130.5	74	4	
145	74	4	42.4
162.5	70	4	38.8
181	68	4	34.9
202	65	4	30.3
222	62	4	28.4
246	55	4	23.8
254	33	4	14
266	22	4	3.8
275	20	4	6.1
290	17	4	5.3
304	15	4	5.2
BDPA OE at 18.8 T			
Temperature (K)	^{1}H Enhancement	Error (±)	^{1}H T_B
121	76	4	90
128	70	4	
140	68	4	76
157	65	4	
175	57	4	55
193	48	4	43
207	43	4	42
230	37	4	35
253	27	4	25
266	25	4	12
275	22	4	12
280	18	4	10
286	16	4	11
BDPA SE at 9.4 T			
Temperature (K)	^{1}H Enhancement	Error (±)	^{1}H T_B
117	140	4	35.5
133	129	4	34
145	120	4	32
162.5	104	4	28.91
181	91	4	25.9
199	76	4	22.8
226	69	4	22

246	64	4	19.7
254	46	4	9.9
264	12	4	2.4

TEKPol CE at 9.4 T			
Temperature (K)	^{1}H Enhancement	Error (±)	^{1}H T_B
119	236	8	1.98
126	215	8	
133	212	8	1.96
145	182	8	
157	162	8	1.88
168	151	8	1.8
183	121	8	1.64
205	98	8	1.51
222	85	8	1.48
240	86	8	1.57
257	74	8	1.28
266	45	8	0.78
274	22	8	0.44
TEKPol CE at 18.8 T			
Temperature (K)	^{1}H Enhancement	Error (±)	^{1}H T_B
124	51.6	1.5	3.1
128	48.1	1.5	3.2
156	43.7	1.5	3.1
164	41.2	1.5	3
175	37.7	1.5	2.7
187	36	1.5	2.6
209	29	1.5	2.2
215	26.5	1.5	2.1
227	22.7	1.5	2
235	17.6	1.5	1.8
256	14.3	1.5	1.7
262	9	1.5	1.2
271	5.6	1.5	0.92

References

1. Rossini, A. J.; Zagdoun, A.; Lelli, M.; Gajan, D.; Rascón, F.; Rosay, M.; Maas, W. E.; Copéret, C.; Lesage, A.; Emsley, L. *Chem. Sci.* **2011**, *3*, 108–115.
2. Zagdoun, A.; Casano, G.; Ouari, O.; Schwarzwälder, M.; Rossini, A. J.; Aussenac, F.; Yulikov, M.; Jeschke, G.; Copéret, C.; Lesage, A.; Tordo, P.; Emsley, L. *J. Am. Chem. Soc.* **2013**, *135*, 12790–12797.
3. Zagdoun, A.; Rossini, A. J.; Gajan, D.; Bourdolle, A.; Ouari, O.; Rosay, M.; Maas, W. E.; Tordo, P.; Lelli, M.; Emsley, L.; Lesage, A.; Copéret, C. *Chem. Commun.* **2012**, *48*, 654–656.
4. Zagdoun, A.; Casano, G.; Ouari, O.; Lapadula, G.; Rossini, A. J.; Lelli, M.; Baffert, M.; Gajan, D.; Veyre, L.; Maas, W. E.; Rosay, M.; Weber, R. T.; Thieuleux, C.; Copéret, C.; Lesage, A.; Tordo, P.; Emsley, L. *J. Am. Chem. Soc.* **2012**, *134*, 2284–2291.
5. Can, T. V.; Caporini, M. A.; Mentink-Vigier, F.; Corzilius, B.; Walish, J. J.; Rosay, M.; Maas, W. E.; Baldus, M.; Vega, S.; Swager, T. M.; Griffin, R. G. *J. Chem. Phys.* **2014**, *141*, 064202.
6. Rosay, M.; Tometich, L.; Pawsey, S.; Bader, R.; Schauwecker, R.; Blank, M.; Borchard, P. M.; Cauffman, S. R.; Felch, K. L.; Weber, R. T.; Temkin, R. J.; Griffin, R. G.; Maas, W. E. *Phys. Chem. Chem. Phys.* **2010**, *12*, 5850–5860.
7. Concistrè, M.; Carignani, E.; Borsacchi, S.; Johannessen, O. G.; Mennucci, B.; Yang, Y.; Geppi, M.; Levitt, M. H. *J. Phys. Chem. Lett.* **2014**, *5*, 512–516.
8. Thurber, K. R.; Tycko, R. *J. Magn. Reson.* **2009**, *196*, 84–87.
9. Rossini, A. J.; Zagdoun, A.; Hegner, F.; Schwarzwälder, M.; Gajan, D.; Copéret, C.; Lesage, A.; Emsley, L. *J. Am. Chem. Soc.* **2012**, *134*, 16899–16908.
10. Rossini, A. J.; Widdifield, C. M.; Zagdoun, A.; Lelli, M.; Schwarzwälder, M.; Copéret, C.; Lesage, A.; Emsley, L. *J. Am. Chem. Soc.* **2014**, *136*, 2324–2334.
11. Mollica, G.; Dekhil, M.; Ziarelli, F.; Thureau, P.; Viel, S. *Angew. Chem. Int. Ed. Engl.* **2015**, *54*, 6028–6031.
12. Takahashi, H.; Hediger, S.; De Paëpe, G. *Chem. Commun.* **2013**, *49*, 9479.
13. Fung, B. M.; Khitrin, A. K.; Ermolaev, K. *J. Magn. Reson.* **2000**, *142*, 97–101.
14. van der Wel, P. C. A.; Hu, K.-N.; Lewandowski, J.; Griffin, R. G. *J. Am. Chem. Soc.* **2006**, *128*, 10840–10846.
15. Ong, T.-C.; Mak-Jurkauskas, M. L.; Walish, J. J.; Michaelis, V. K.; Corzilius, B.; Smith, A. A.; Clausen, A. M.; Cheetham, J. C.; Swager, T. M.; Griffin, R. G. *J. Phys. Chem. B* **2013**, *117*, 3040–3046.
16. Paleari, D.; Rossi, G. A.; Nicolini, G.; Olivieri, D. *Expert Opin. Drug Discov.* **2011**, *6*, 1203–1214.
17. Carignani, E.; Borsacchi, S.; Geppi, M. *J. Phys. Chem. A* **2011**, *115*, 8783–8790.
18. Concistrè, M.; Johannessen, O. G.; Carignani, E.; Geppi, M.; Levitt, M. H. *Acc. Chem. Res.* **2013**, *46*, 1914–1922.
19. The uncertainty in determining the enhancement in the IBU-S resonances is due to the weak signal to noise ratio in the spectrum without microwaves. Enhancements about 8 to 13 are observed for different ^{13}C resonances that might suggest a different distribution of the polarization due to the dynamics in the crystal. ε_{C_CP} for IBU-S at higher temperature could not be accurately measured because of the broadening of the signals (especially up to 177 K) that makes the spectrum without microwave too weak to provide an accurate reference.

20. Pinon, A. C.; Rossini, A. J.; Widdifield, C. M.; Gajan, D.; Emsley, L. *Mol. Pharm.* **2015,** DOI: 10.1021/acs.molpharmaceut.5b00610.
21. Rossini, A. J.; Schlagnitweit, J.; Lesage, A.; Emsley, L. *J. Magn. Reson.* **2015**, *259*, 192–198.
22. Abragam, A. *The Principles of Nuclear Magnetism*; Oxford University Press, **1961**.
23. Abragam, A.; Goldman, M. *Rep. Prog. Phys*. **1978**.
24. Abragam, A.; Goldman, M. *Nuclear Magnetism: Order and Disorder*; Clarendon Press - Oxford : New York, **1982**.
25. Smith, A. A.; Corzilius, B.; Barnes, A. B.; Maly, T.; Griffin, R. G. *J. Chem. Phys.* **2012**, *136*, 015101.
26. Corzilius, B.; Smith, A. A.; Griffin, R. G. *J. Chem. Phys.* **2012**, *137*, 054201.
27. Hovav, Y.; Feintuch, A.; Vega, S. *J. Magn. Reson.* **2010**, *207*, 176–189.
28. Thurber, K. R.; Tycko, R. *Isr. J. Chem.* **2014**, *54*, 39–46.
29. Thurber, K. R.; Tycko, R. *J. Chem. Phys.* **2014**, *140*, 184201–184201.
30. Becerra, L. R.; Gerfen, G. J.; Temkin, R. J.; Singel, D. J.; Griffin, R. G. *Phys. Rev. Lett.* **1993**, *71*, 3561–3564.
31. Wind, R. A.; Duijvestijn, M. J.; Van Der Lugt, C.; Manenschijn, A.; Vriend, J. *Prog. Nucl. Magn. Reson. Spectrosc.* **1985**, *17*, 33–67.
32. Duijvestijn, M. J.; Wind, R. A.; Smidt, J. *Physica B,* **1986,** *138,* 147–170.
33. Can, T. V.; Ni, Q. Z.; Griffin, R. G. *J. Magn. Reson.* **2015**, *253*, 23–35.
34. Hausser, K. H.; Stehlik, D. *Adv. Magn. Reson.* **1968**, *3*, 79–139.
35. Müller-Warmuth, W.; Meise-Gresch, K. *Adv. Magn. Reson.* **1983**, *11*, 1–45.
36. Griesinger, C.; Bennati, M.; Vieth, H. M.; Luchinat, C.; Parigi, G.; Höfer, P.; Engelke, F.; Glaser, S. J.; Denysenkov, V.; Prisner, T. F. *Prog. Nucl. Magn. Reson. Spectrosc.* **2012**, *64*, 4–28